Available online at www.sciencedirect.com

ScienceDirect

journal homepage: www.elsevier.com/locate/he

Preparation of $CoMo/Al_2O_3$, $CoMo/CeO_2$, $CoMo/TiO_2$ catalysts using ultrasonic spray pyrolysis for the hydro-desulfurization of 4, 6-dimethyldibenzothiophene for fuel cell applications

Hyun Koo Kim [a,b,1], *Chang-Whan Lee* [a,1], *Minsoo Kim* [a], *Joo Hyeng Oh* [a], *Shin Ae Song* [c], *Seong-Cheol Jang* [a], *Chang Won Yoon* [a], *Jonghee Han* [a], *Sung Pil Yoon* [a], *Suk Woo Nam* [a], *Dae-Ki Choi* [a], *Yong-gun Shul* [b], *Hyung Chul Ham* [a,*]

[a] *Fuel Cell Research Center, Korea Institute of Science and Technology (KIST), Hwarangno 14-gil 5, Seongbuk-gu, Seoul 136-791, Republic of Korea*

[b] *Department of Chemical and Biomolecular Engineering, Yonsei University, 50 Yonsei-ro, Seodaemun-gu, Seoul 120-749, South Korea*

[c] *Micro/Nano Scale Manufacturing Group, Korea Institute of Industrial Technology, 143 Hanggaulro, Sangnok-gu, Ansan-si, Gyeonggi-do, 426-910, Republic of Korea*

ARTICLE INFO

Article history:
Received 25 December 2015
Received in revised form
31 May 2016
Accepted 1 June 2016
Available online 30 June 2016

Keywords:
Ultrasonic spray pyrolysis (USP)
Hydrodesulfurization
4, 6-dimethyldibenzothiophene (4, 6-DMDBT)
Catalyst support
Fuel cell

ABSTRACT

One of promising methods for removing the sulfur compounds from diesel fuel is hydrodesulfurization, in which the sulfur in diesel is hydrotreated by reaction with H_2 to liberate H_2S. In hydrodesulfurization, a highly efficient catalyst is required fuel cell applications because the level of sulfur compounds should be below 0.1 ppm to allow stable molten carbonate fuel cell operation. In this study, we prepared the $CoMo/Al_2O_3$, $CoMo/CeO_2$, $CoMo/TiO_2$ catalysts using ultrasonic spray pyrolysis and the activities of synthesized catalysts toward the hydrodesulfurization of 4, 6-dimethyldibenzothiophene were examined using a flow reactor. First, our measurement results using X-ray diffraction, scanning electron microscope, field emission gun electron probe micro analyzer and transmission electron microscope suggested that the Co and Mo particles are uniformly distributed on the supports (Al_2O_3, CeO_2, and TiO_2) we considered. Second, from the analysis of surface properties using via Raman spectroscopy, we identified the characteristic phases (such as $Ce_2Mo_3O_{13}$, MoO_3, and $CoMoO_4$) of each synthesized catalyst, which may significantly influence hydrodesulfurization reactivity. Finally, the evaluation of catalytic activity showed that the order of hydrodesulfurization activity is $CoMo/CeO_2 > CoMo/Al_2O_3 > CoMo/TiO_2$. In particular, a $CoMo/CeO_2$ catalyst exhibits the highest catalytic activity toward hydrodesulfurization, reducing the amount of 4, 6-dimethyldibenzothiophene from 10 ppm to about 0.1 ppm at 350 °C.

* *Corresponding author*. Tel.: +82 2 958 5889; fax: +82 2 958 5199.
E-mail address: hchahm@kist.re.kr (H.C. Ham).

[1] These authors contributed equally to this work.

http://dx.doi.org/10.1016/j.ijhydene.2016.06.040

Nomenclatures

4, 6-DMDBT	4, 6-dimethyldibenzothiophene
ADS	Adsorptive desulfurization
BPR	Back Pressure Regulator
CMA	CoMo particles supported on Al_2O_3
CMC	CoMo particles supported on CeO_2
CMO	CoMo particles without support
CMT	CoMo particles supported on TiO_2
DBT	Dibenzothiophene
DDS	Direct Desulfurization
FE-EPMA	Field Emission Gun Electron Probe Micro Analyzer
GC-SCD	Gas Chromatography Sulfur Chemiluminescence Detector
HDS	Hydro-desulfurization
LHSV	Liquid Hourly Space Velocity
ODS	oxidative desulfurization
SEM	scanning electron microscope
TEM	transmission electron microscope
USP	Ultrasonic spray pyrolysis
XRD	X-ray Diffraction

Introduction

Regulations on sulfur levels in diesel fuels have become increasingly strict over the years and therefore, development of active catalysts for desulfurization has always been a key issue. The emissions such as SO_x, NO_x, and CO_x are typical pollutants which are under heavy regulation [1]. The current sulfur level of diesel fuels in Korea is below 10 ppm and the development of desulfurization techniques has been constantly progressing [2].

In addition, diesel is a good candidate as a hydrogen source since it can yield the largest amount of methane when passed through a pre-reformer. It can also be used as a hydrogen source for fuel cells such as proton exchange membrane fuel cells (PEMFCs) [3], molten carbonate fuel cells (MCFCs) [4], and solid oxide fuel cells (SOFCs) [5]. However, the organic sulfur present at ppm levels can poison the reforming catalysts [5] and the fuel cell electrodes. Therefore, sulfur content of diesel fuels should be reduced less than 0.1 ppm in order to operate reforming systems and fuel cells safely [6].

The desulfurization processes can be distinguished by the utilization of hydrogen: Adsorptive desulfurization (ADS) [7], oxidative desulfurization (ODS) [8], and hydro-desulfurization (HDS) [9]. HDS is widely used in oil refineries to reduce sulfur content of commercial fuels and is operated at high temperatures (300–400 °C) and high pressures (10–50 bar). HDS has the advantage that it is a continuous process where the catalyst can be used for a long period whereas, in ADS, adsorbents have a certain breakthrough capacity in which regeneration is required when the adsorbent has reached its breakthrough capacity [10,11].

For the HDS process, commercial catalysts such as Co–Mo/Al_2O_3 and Ni–Mo/Al_2O_3 are widely used where Co or Ni enhances activities of catalysts by acting on the edge plane of MoS_2 [12–14]. For support structures of commercial catalysts, γ-Al_2O_3 is widely used because the OH group on the surface of Al_2O_3 strongly interacts with the OH groups on the MoO_2 surface, leading to the modification of electronic structure in catalytic surface.

The conventional synthesis methods for the commercial desulfurization catalysts are homogeneous sulfide precipitation (HSP), impregnation, and co-precipitation [15]. In recent years, ultrasonic spray pyrolysis (USP) has been applied to the preparation of superior catalysts, which may greatly impact selectivity and reactivity [16]. USP is a technique where a metal precursor solution is vaporized by ultrasonic waves into micro-sized droplets, which are carried down to a high temperature furnace (500–900 °C) for crystallization. USP has following advantages; preparation of the precursor solution is easy, it is a continuous process, multi-component materials can be synthesized, and experimental parameters such as temperature and reaction time can be controlled easily [17].

In this study, the catalysts such as CoMo/Al_2O_3, CoMo/CeO_2 and CoMo/TiO_2 for the HDS process was synthesized by the USP process in order to reduce the sulfur level of diesel to the acceptable level of fuel cell application (about 0.1 ppm). After that, the physical properties and surface characteristics of synthesized catalysts were investigated through SEM

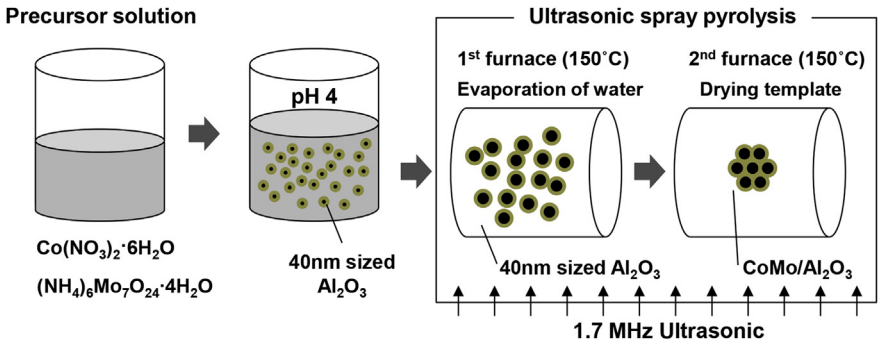

Fig. 1 – Synthesis of CoMo/Al_2O_3 catalysts in ultrasonic spray pyrolysis.

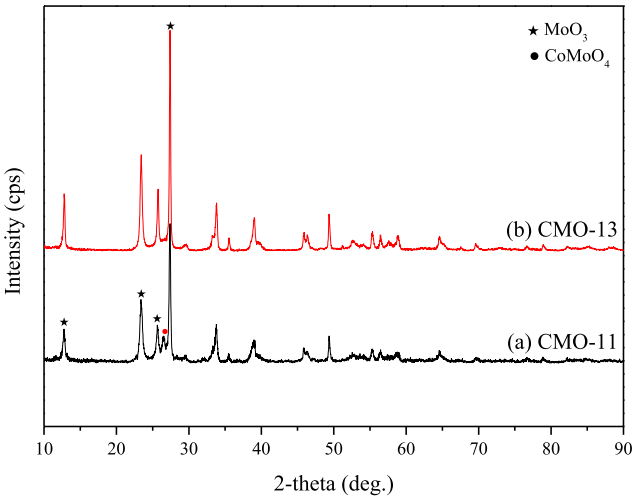

Fig. 2 – XRD patterns of (a) CMO-11 and (b) CMO-13.

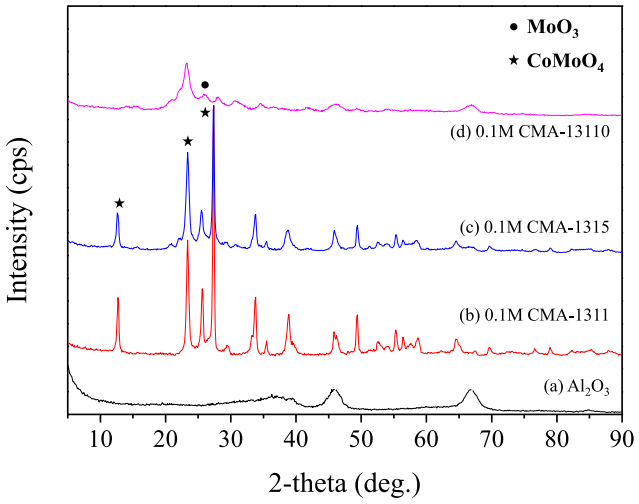

Fig. 4 – XRD patterns of (a) Al_2O_3, (b) CMA-1311, (c) CMA-1315 and (d) CMA-13110.

(scanning electron microscope) images, XRD (X-ray diffraction), and Raman spectroscopy. Finally, the activity of prepared catalysts toward HDS was evaluated using a flow reactor with a model diesel. A model diesel was fabricated adding 4, 6-Dimethyldibenzothiophene (4, 6-DMDBT) in dodecane with the concentration of 10 ppm.

Experiments

Catalyst preparation

NiMo or CoMo-based catalyst which has higher stability is widely used in the HDS process. In this study, CoMo doped catalysts were synthesized on different supports by the USP process. Commercial support which increases the activity of the catalyst at high oxygen storage capacity (γ-Al_2O_3, TiO_2, and CeO_2) were used.

Synthesis process of catalyst is divided into 2 stages. At first, precursors were synthesized. After that, the catalyst powders were synthesized by using the precursor through the USP process. The USP process employs ultrasonic for precursor solution distracted to micro sol. After that, the solvent evaporates in the high temperature tubular furnace. The metal precursors in solution are acquired rapidly at exit filter by crystallization.

For the description of the synthesis method of catalysts, CoMo with the support of Al_2O_3 ($CoMo/Al_2O_3$) was selected as an example. The precursor solution was prepared by adding cobalt nitrate hexahydrate [$Co(NO_3)_2 \cdot 6H_2O$, Junsei, 98.9%] and ammonium heptamolybdate tetrahydrate [$(NH_4)_6Mo_7O_{24}$ $4H_2O$, Junsei, 99%] in deionized water (DIW) at molar ratios of 1:1, 1:3, and 1:5 and diluting to a concentration of 0.1 M.

After that, catalysts for the HDS process were synthesized using precursors. The synthesis of $CoMo/Al_2O_3$ catalysts using the UPS process is shown in Fig. 1. The prepared CoMo

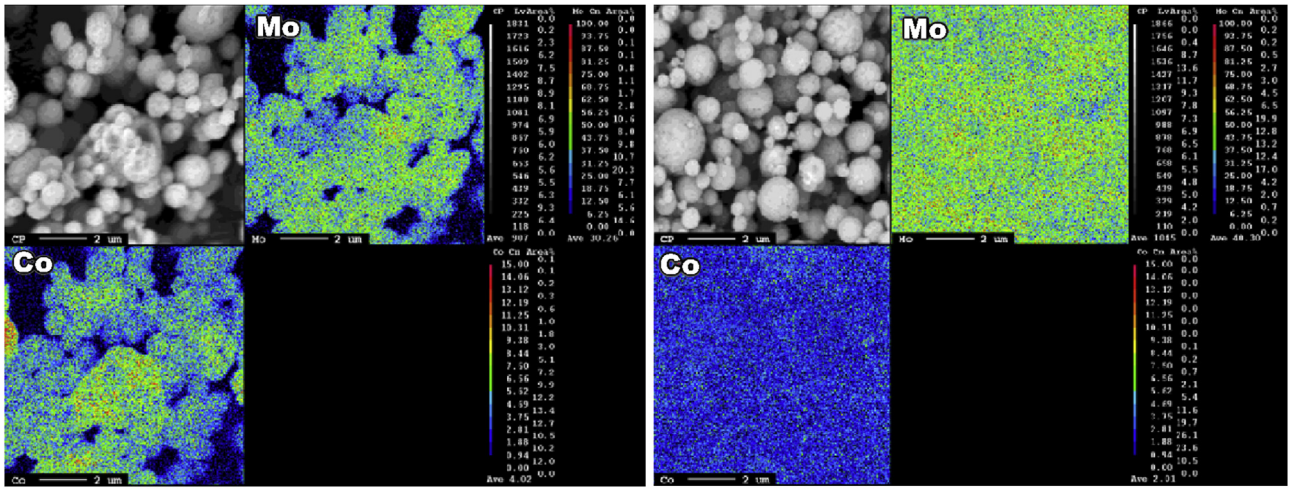

Fig. 3 – EPMA images of (a) CMO-11 and (b) CMO-13.

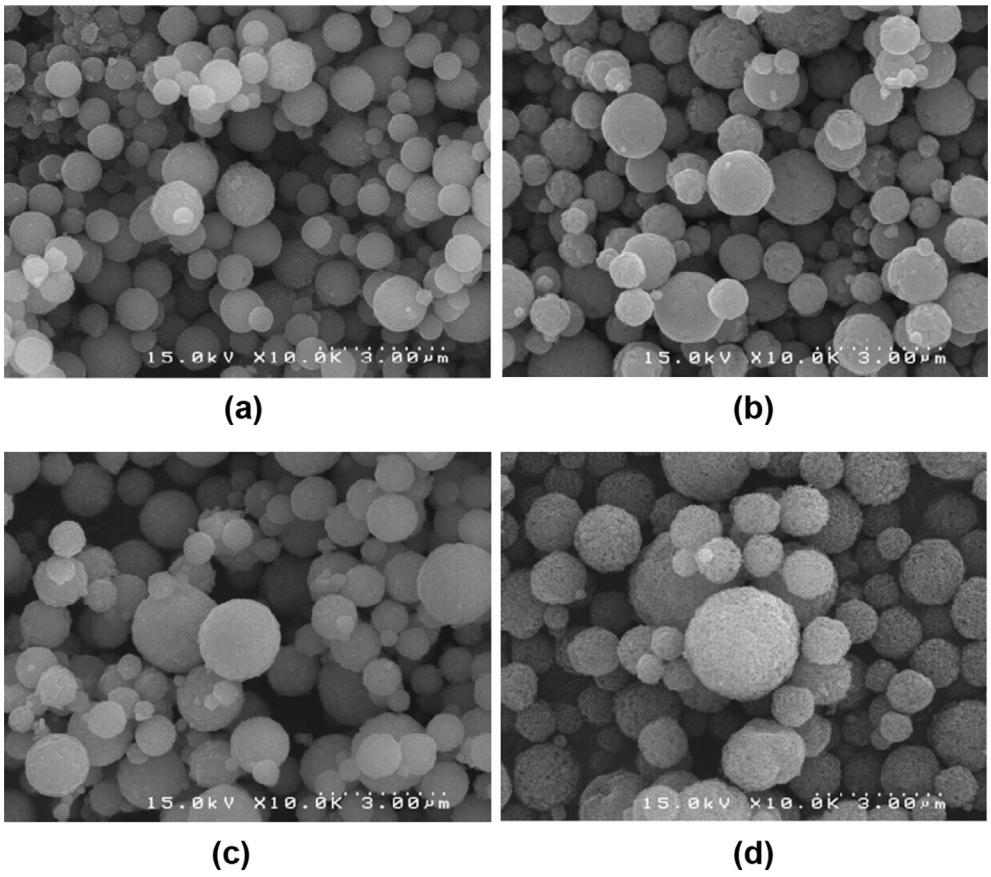

Fig. 5 – SEM images of (a) Al_2O_3, (b) CMA-1311, (c) CMA-1315 and (d) CMA-13110.

precursor solution was mixed with a colloidal solution of support. The colloidal solutions were γ-phase aluminum oxide [40 nm sized Al_2O_3 20% in H_2O, colloidal dispersion, Alfa Aesar, pH 4], cerium oxide [10–20 nm sized CeO_2 20% in H_2O, colloidal dispersion, Alfa Aesar, pH 2], and titanium (IV) oxide colloidal dispersion [TiO_2, 20–35% in H_2O colloidal dispersion, Alfa Aesar, pH 8]. The colloidal solutions were inserted into the USP process. Using the USP process, CoMo/Al_2O_3 was synthesized.

The synthesized catalysts by the USP process were denoted in terms of the materials used and their component ratio, for example, CMA-13110 is CoMo supported on Al_2O_3 with Co: Mo mole ratio 1:3 and Mo and Al_2O_3 mole ratio 1:10. For this research, CoMo ratios were fixed to 1:3 whereas the mole ratios for Mo and support were 1:1, 1:5, and 1:10.

Hydrodesulfurization (HDS) reaction

Diesel fuel contains more organic sulfur compounds than gasoline and jet fuel; as a result, diesel has a higher boiling point. The organic sulfur compounds in commercial diesel are primarily thiophene-based organics. These thiophenes may have one or more methyl groups, or more than one benzo group. Thiophenes with two benzo groups are called dibenzothiophene (DBT), which is the most common form of refractory organic sulfur matter. DBT can have alkyl groups attached to the benzo groups, which create steric hindrance

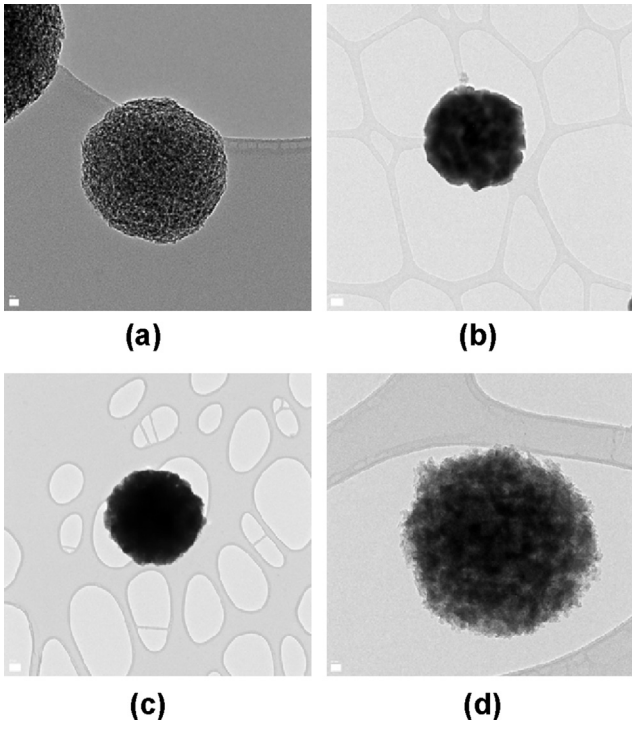

Fig. 6 – TEM images of (a) Al_2O_3, (b) CMA-1311, (c) CMA-1315 and (d) CMA-13110.

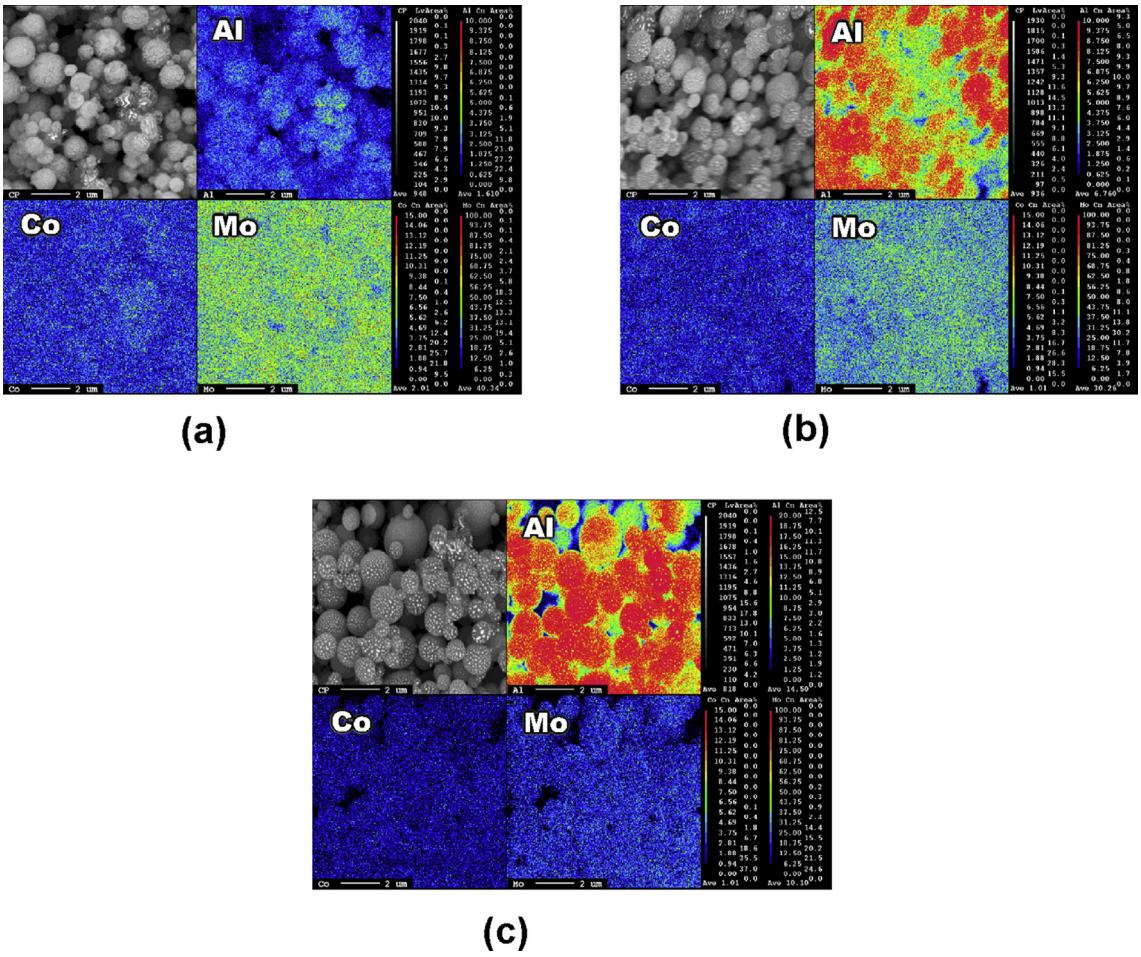

Fig. 7 – EPMA images of (a) CMA-1311, (b) CMA-1315, and (c) CMA-13110.

around the sulfur atom [18]. The dimethylated DBT, known as dimethyldibenzothiophene (DMDBT), is the typical refractory alkylated DBT. Among DMDBT, 4, 6-DMDBT exhibited the lowest desulfurization rate [14].

In the experiments, model diesel was used instead of commercial diesel. Model diesel was prepared by adding 4, 6-dimethyldibenzothiophene (4, 6-DMDBT, 97%, Sigma–Aldrich) to dodecane (Kanto Chemical). The model diesel consisted of 4, 6-DMDBT as the sulfur compound and dodecane as the solvent. As the sulfur level in commercial diesel is below 10 ppm, 10 ppm of 4, 6-DMDBT was added to dodecane to make a model diesel solution. Sulfur content analysis was carried out using GC-SCD using ASTM D 5623-94 which allows sulfur detection in the range of 0.1–100 ppm. The catalyst was activated by pretreatment with 5% H_2S/H_2 at 400 °C for 2 h. The products of the HDS process passed through the BPR and were separated into hydrogen, H_2S, and desulfurized diesel.

Catalyst characterization

X-ray diffraction (XRD, Rint/DMAX-2000, Rigaku), scanning electron microscope (SEM, FEI Nova 200), transmission electron microscope (TEM, FEI TitanTM 80–300), nitrogen adsorption/desorption method (Autosorb-iQ 2ST/MP Quantachrome), Raman spectroscopy (Renishaw In Via Raman Microscope), Field Emission Gun Electron Probe Micro Analyzer (FEG-EPMA, JEOL JXA-8500F), and GC-SCD were used for physical study of the prepared catalysts and desulfurized model diesel.

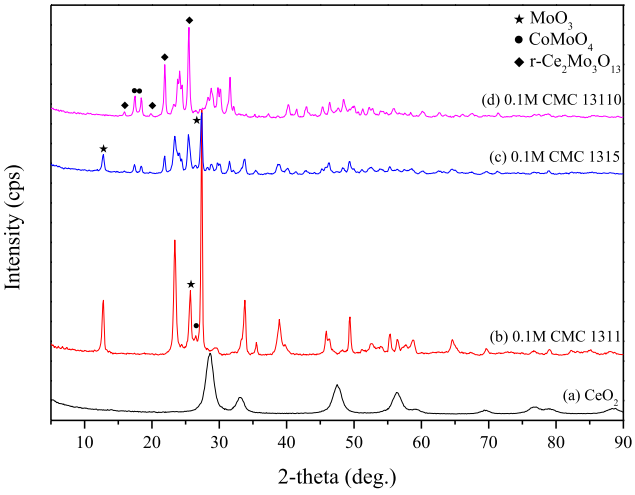

Fig. 8 – XRD patterns of (a) CeO_2, (b) CMC-1311, (c) CMC-1315 and (d) CMC-13110.

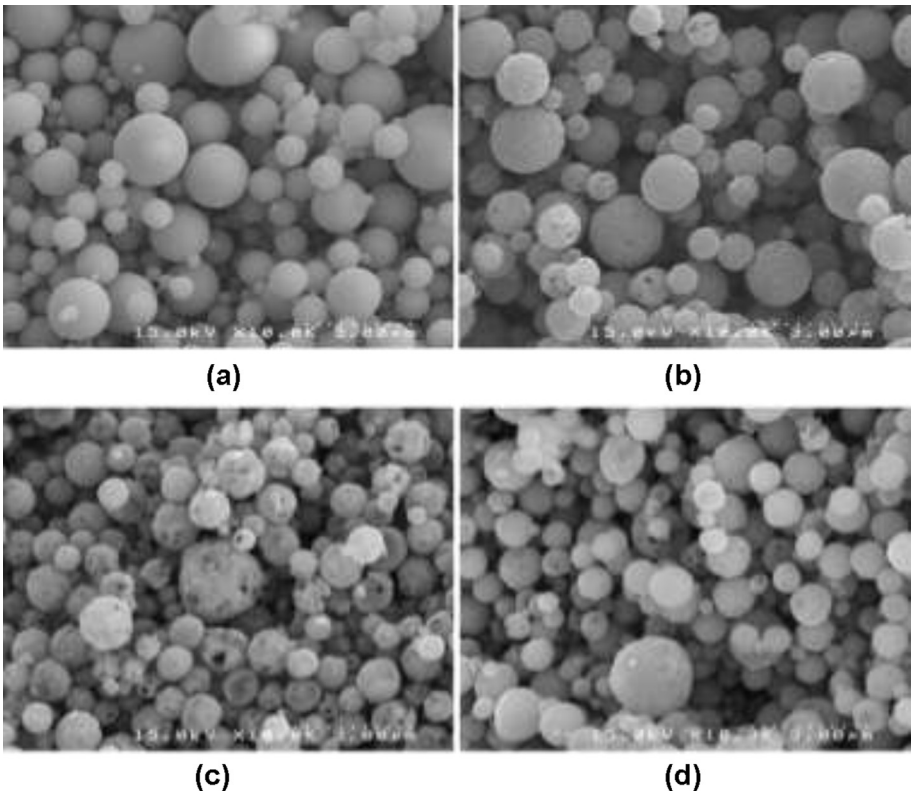

Fig. 9 – SEM images of (a) CeO_2, (b) CMC-1311, (c) CMC-1315 and (d) CMC-13110.

Desulfurization experiments use high resolution gas chromatography (GC) to study the sulfur content. The commonly known detectors of sulfur are a flame photometric detector (FPD), an atomic emission detector (AED) and a sulfur chemiluminescence detector (SCD) [19]. In this research, gas chromatography with a sulfur chemiluminescence detector (GC-SCD) used to analyze sulfur content because it is known to be the most sensitive and, capable method for detecting sulfur at 0.1 ppm levels.

Results and discussion

CoMo particles without oxide materials (supports)

$CoMoO_4$ particles were prepared with Co:Mo molar ratios of 1:1 and 1:3. For example, CMO-11 and CMO-13 mean the $CoMoO_4$ particles with Co:Mo molar ratios of 1:1 and 1:3, respectively. XRD patterns in Fig. 2 show coexistence of MoO_3 and $CoMoO_4$ in CMO-11 and CMO-13. The MoO_3 peak in CMO-13 was more intense than in CMO-11 because of a higher Mo content in CMO-13. The XRD patterns were compared with reference data, JCPDS 00-001-0706 for MoO_3 and JCPDS 00-021-0868 for $CoMoO_4$. MoO_3 peaks were found at 14.5°, 27.3° and 28.2°, whereas a $CoMoO_4$ peak was found at 26.5° which confirmed that USP-synthesized particles were mixtures of MoO_3 and $CoMoO_4$.

Fig. 3 shows the FEG-EPMA images of CMO-11, and CMO-13. FEG-EPMA was analyzed at 1000 magnifications to check the distribution of Co and Mo throughout the catalyst particle

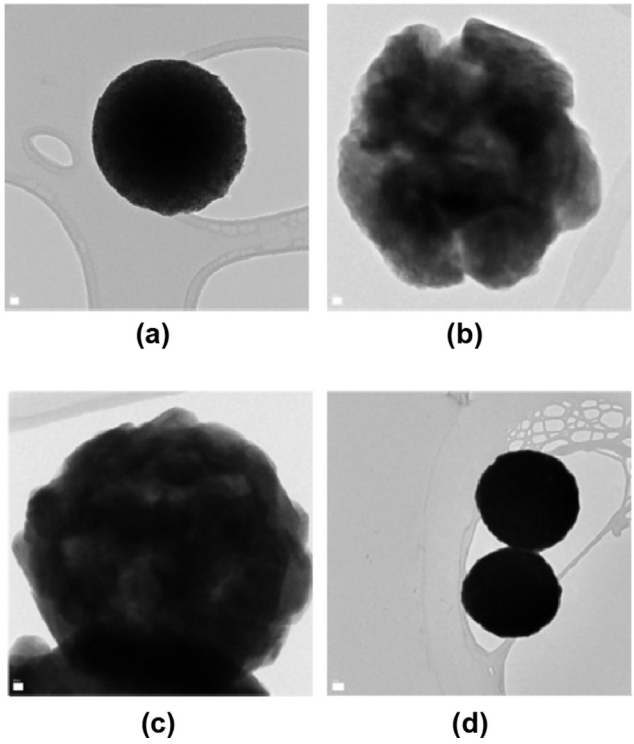

Fig. 10 – TEM images of (a) CeO_2, (b) CMC-1311, (c) CMC-1315 and (d) CMC-13110.

surface. Both CMO-11 and CMO-13 showed even distributions of Co and Mo, but, CMO-13 showed lower concentration of Co due to the lower Co content in the precursor compared to CMO-11. Therefore, catalysts for the HDS process were synthesized with the Co:Mo mole ratio of 1:3.

CoMo particles with Al_2O_3

Fig. 4 shows the XRD patterns for CoMo particles supported on Al_2O_3 (indicated as CMA) with varying Mo support ratios in comparison with that of pure Al_2O_3 support. XRD patterns for neat Al_2O_3 showed low crystallinity and amorphous phase [20]. MoO_3 was found to be the main phase for XRD results of CMA-1311 and CMA-1315. MoO_3 and $CoMoO_4$ peaks were identical to the aforementioned CoMo synthesized without a support. As shown in Fig. 4(d), the XRD pattern of CMA-13110 showed significantly reduced MoO_3 phase due to the large amount of Al_2O_3 support.

The SEM images of the synthesized catalyst particles are shown in Fig. 5. The particles sizes were between 0.1 and 3 μm, as determined by visual inspection. The particles were spherical shape which was identical to the support material, Al_2O_3. Differences in Mo/Al_2O_3 molar ratio (1:1 and 1:3) did not have any effect on the visible particle size or morphology. CMA-13110, which had the largest amount of Al_2O_3, had a porous surface which looked the most similar to neat Al_2O_3. The TEM images of CMA particles are shown in Fig. 6. The particles of CMA-1311 and CMA-1315 appeared dense, whereas CMA-13110 had small pores on the surface due to the high amount of Al_2O_3 relative to CoMo.

FEG-EPMA images of CMA-1311, CMA-1315 and CMA-13110 are presented in Fig. 7. From EPMA images, the distribution and concentration of Co, Mo and Al. Increase in Al content was clearly visible, where CMA-13110 showed the highest concentration of Al throughout the particle surface. This was consistent with the SEM and TEM results showing CMA-13110's porous and fluffy surface which looks similar to Al_2O_3 in raw form. CMA-13110, which has the highest ratio of Al_2O_3, shows more uniformly distributed Co and Mo.

CoMo particles with CeO_2

XRD patterns of CoMo particles supported on CeO_2 (indicated as CMC) are shown in Fig. 8. The Mo/support molar ratios were

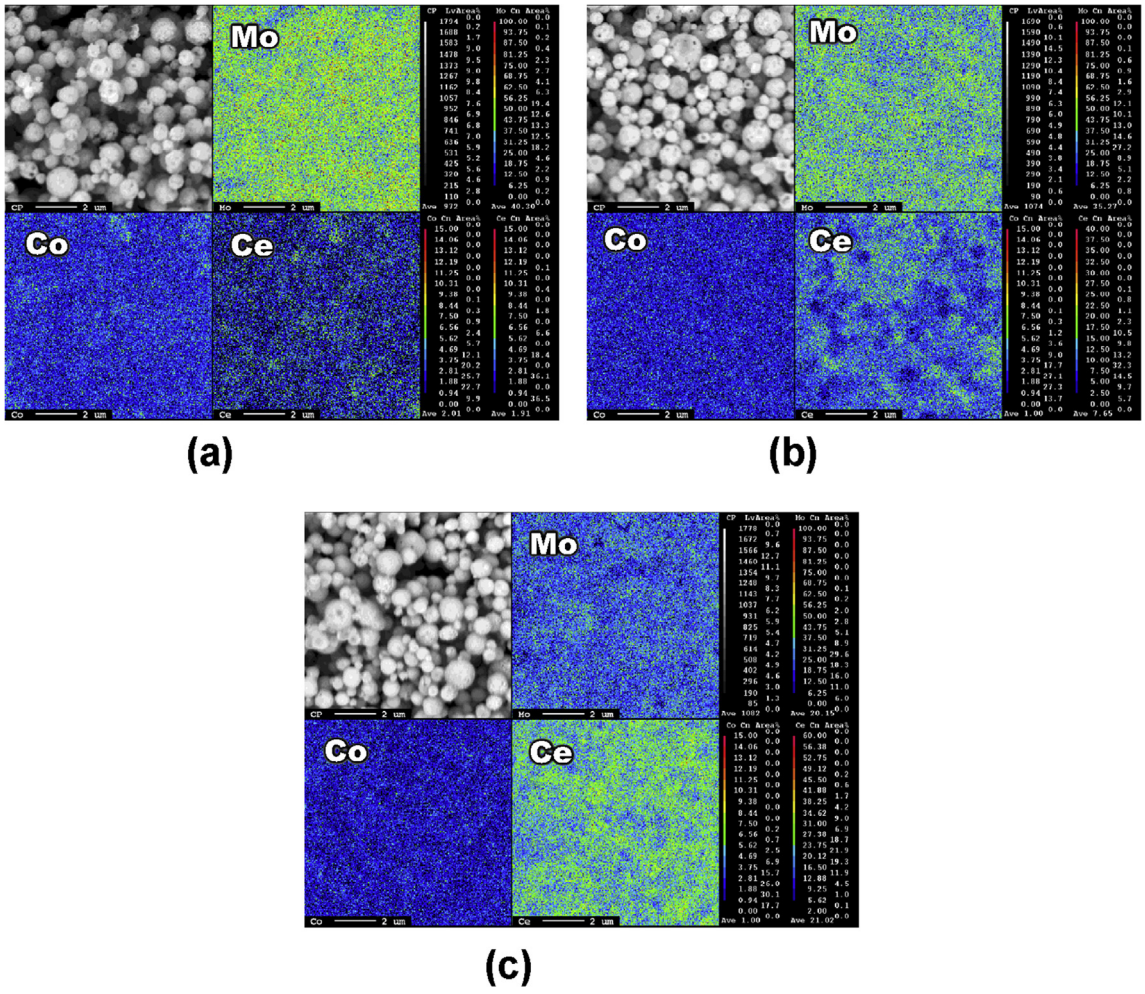

Fig. 11 – EPMA images of (a) CMC-1311, (b) CMC-1315, and (c) CMC-13110.

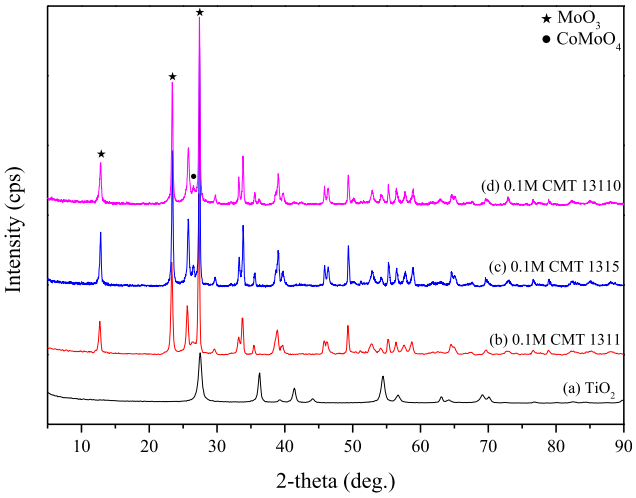

Fig. 12 – XRD patterns of (a) TiO_2, (b) CMT-1311, (c) CMT-1315, and (d) CMT-13110.

1:1, 1:5, and 1:10. MoO_3 was the main phase in CMC-1311 and $CoMoO_4$ peaks were relatively smaller. MoO_3 phase was lower in CMC-1315 where $CoMoO_4$ began to appear. Two different types of $CoMoO_4$ were made for the case of CMC-1315 and CMC-13110.

Fig. 9 shows SEM images of CMC particles. Pores were seen on the surface of all three CMC particles, with CMC-1315 appearing to be the most porous. The pore sizes differed from particles to particles and they were irregularly shaped. Fig. 10 is TEM images of CMC particles. CMC-13110 appeared dense which was identical to neat CeO_2. The CMC particles were spherical with a size range of 0.1–2 μm determined by visual inspection. FEG-EPMA images of CMC particles are shown in Fig. 11. All three CMC particles showed even distributions of Co, Mo and Al.

CoMo particles with TiO_2

Fig. 12 shows the XRD patterns of CoMo particles supported on TiO_2 (indicated as CMT) by varying the ratio of Mo/support and that of pure TiO_2. In the XRD patterns, CMT-1311, CMT-1315, and CMT-13110 were predominantly MoO_3 phase and a small portion was $CoMoO_4$ phase.

Fig. 13 shows the CMT particles' SEM images. Fig. 13(b) shows spherical particles with a rough surface. In Fig. 13(c), spherical and rod shapes coexisted, resulting in a lower surface area. No spherical particles were present in Fig. 13(d). Fig. 14 presents TEM images of the CMT particles. The rod shaped particles seen in Fig. 14(c) and (d) were found to be MoO_3 determined by TEM composition analysis. FEG-EPMA images of the CMT particles are shown in Fig. 15, where (a) and (b) showed even distribution of Co, Mo and Ti. In Fig. 15(c), large amounts of Ti were observed due to high ratio of TiO_2 in the particles.

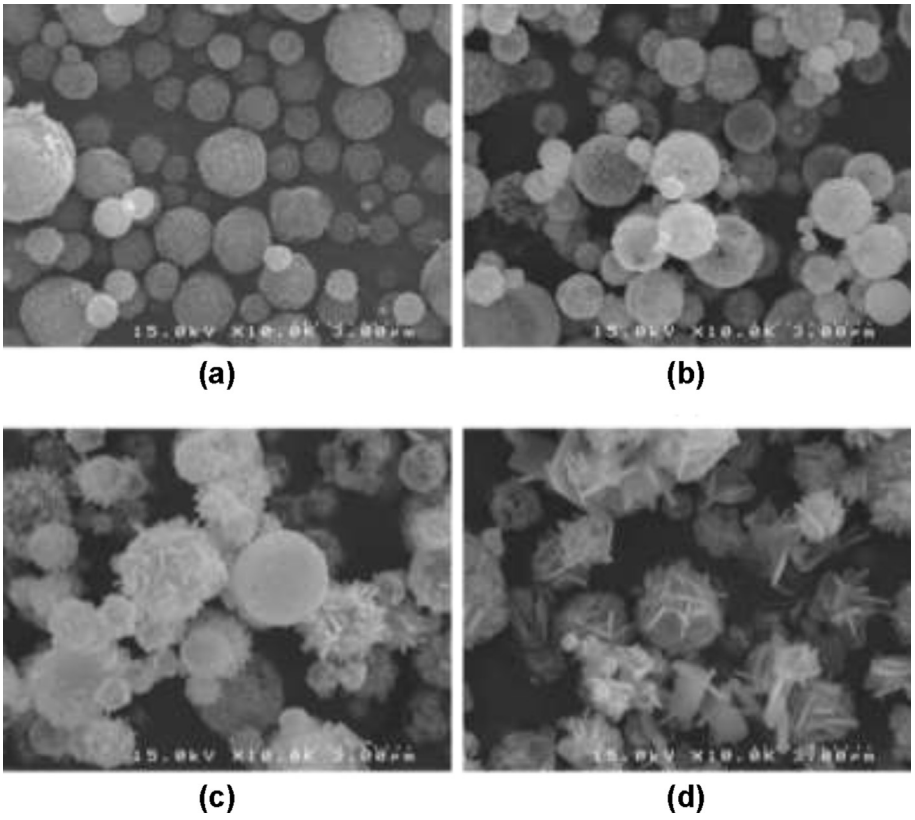

Fig. 13 – SEM images of (a) TiO_2, (b) CMT-1311, (c) CMT-1315, (d) CMT-13110.

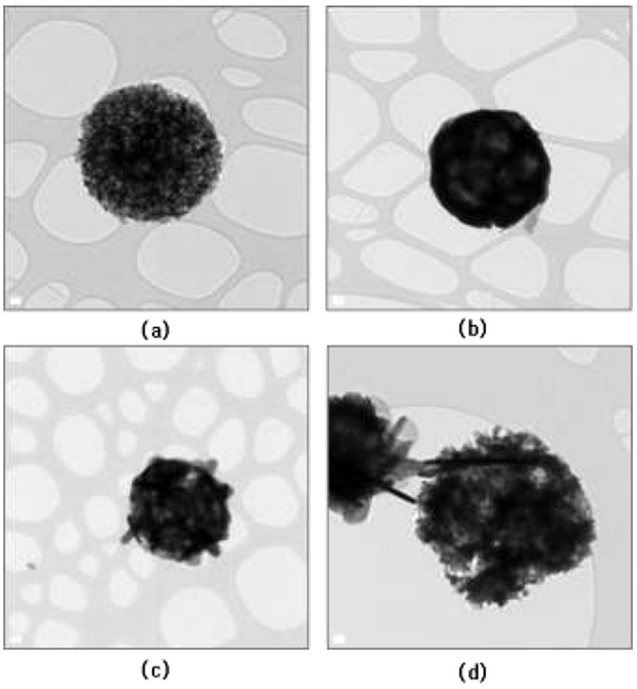

Fig. 14 – TEM images of (a) TiO_2 (b) CMT-1311, (c) CMT-1315, (d) CMT-13110.

Surface properties of CoMo-based catalysts

CMA-13110, CMC-13110, CMT-13110 catalysts were chosen for the candidate for HDS experiments, because Co and Mo are uniformly distributed in the catalysts. Before HDS experiments, surface properties of synthesized catalysts were investigated through Raman spectroscopy. Fig. 16(a), (b), (c), (d), and (e) show the Raman spectras of commercial CoMo/Al_2O_3, CMO-13 (CoMo prepared without oxide materials), CMA-13110 (CoMo/Al_2O_3), CMC-13110 (CoMo/CeO_2), and CMT-13110 (CoMo/TiO_2). CMO-13, CMA-13110, CMC-13110, and CMT-13110 were fabricated by the USP process.

For the CMA-13110 (CoMo/Al_2O_3) case [Fig. 16(c)], we found the characteristic broad bands of MoO_3 phase (995, 819, and 375 cm^{-1}). Here, 995 cm^{-1} is related to the terminal Mo=O vibration, while 819 and 375 cm^{-1} are assigned to the asymmetric Mo–O–Mo stretching vibrations and bending of terminal Mo=O, respectively. In addition, we observed the peak at 939 cm^{-1}, indicating the formation of $CoMoO_4$ phase [21].

For the CMC-13110 (CoMo/CeO_2) [Fig. 16(d)], we identify the strong peaks of $CoMoO_4$ phase (939 cm^{-1}), γ-$Ce_2Mo_3O_{13}$ phase (767 cm^{-1}), and Mo cluster (700 cm^{-1}) [12], while the weak peaks of MoO_3 phase (995, 819, 375 cm^{-1}). This suggests that the mixture of $CoMoO_4$ phase, γ-$Ce_2Mo_3O_{13}$ phase, and Mo

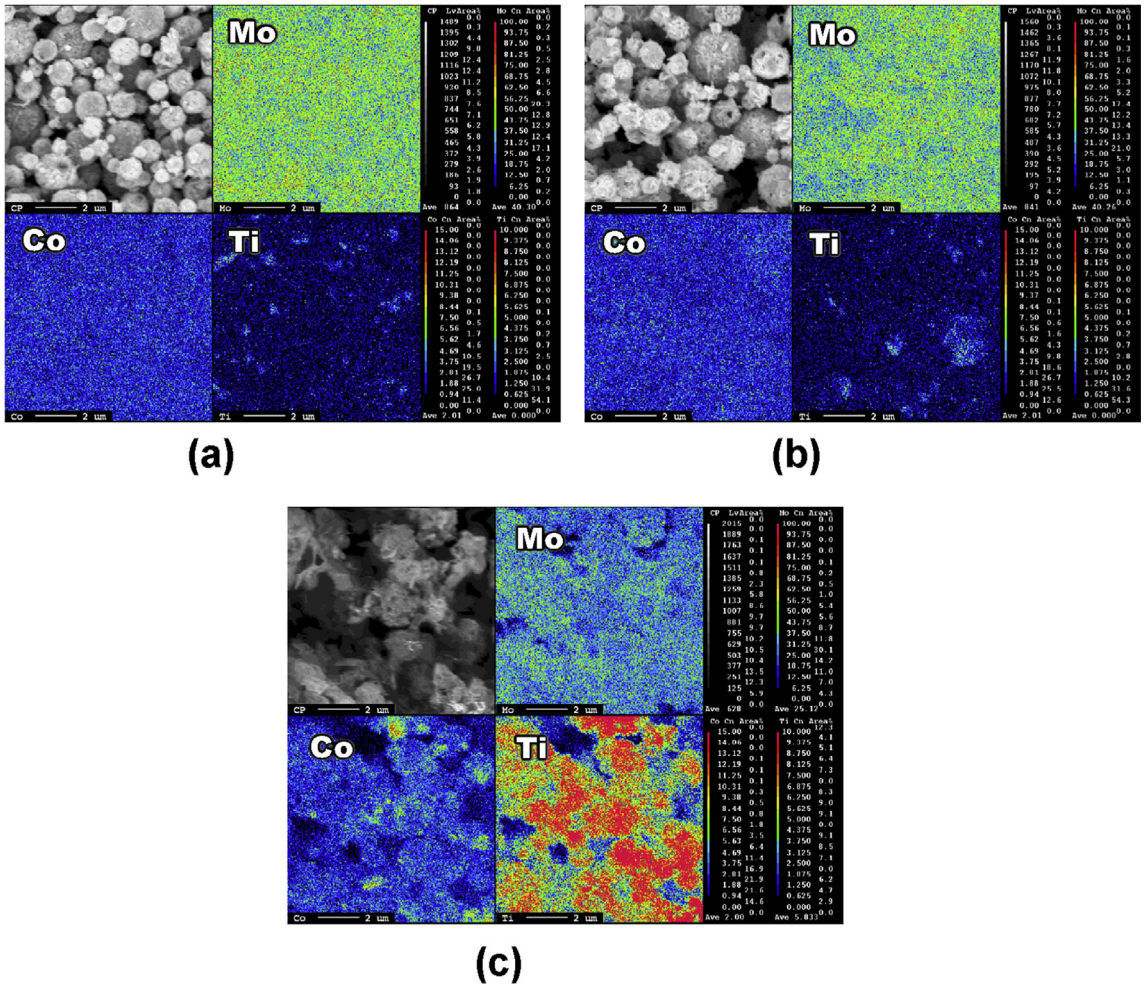

Fig. 15 – EPMA images of (a) CMT-1311, (b) CMT-1315, and (c) CMT-13110.

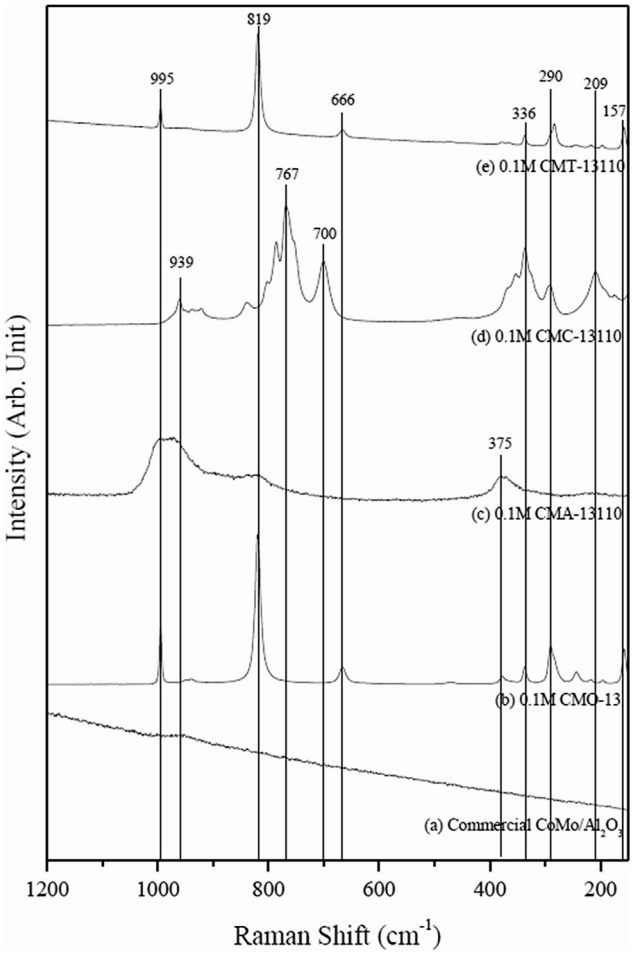

Fig. 16 – Raman spectra of bimetallic oxides samples: (a) commercial $CoMo/Al_2O_3$, (b) CMO-13, (c) CMA-13110, (d) CMC-13110, and (e) CMT-13110.

cluster are dominantly present on the surface of $CoMo/CeO_2$ particle.

Fig. 16(e) shows the Raman spectrum of the CMT-13110 ($CoMo/TiO_2$). We mainly observed the sharp peaks of MoO_3 phase around 995 cm^{-1} (the terminal Mo=O vibration), 336 cm^{-1} (bending of terminal Mo=O), and 290 cm^{-1} the terminal Mo=O vibration), 819 cm^{-1} (the asymmetric Mo–O–Mo stretching vibrations), 666 cm^{-1} (asymmetric Mo–O–Mo stretching vibrations), 336 cm^{-1} (bending of terminal Mo=O), and 290 cm^{-1} (the bridging Mo=O deformation) on the surface of particle on the surface of particle [12,22]. The Raman spectrum of CMO-13 presented in Fig. 16(b) showed sharp peaks of 995 cm^{-1}, 819 cm^{-1}, 666 cm^{-1}, 336 cm^{-1} and 290 cm^{-1}. The Raman spectrum of CMO-13 in Fig. 16(b) is very similar with the Raman spectrum of CMT-13110.

Experimental results of hydrodesulfurization

Model diesel made from 4, 6-DMDBT was desulfurized using commercial $CoMo/Al_2O_3$, CMO-13, CMA-13110, CMC-13110, and CMT-13110 at temperatures 350 °C and 400 °C. The liquid hourly space velocity (LHSV) was 2.1 hr^{-1}. The catalysts CMO-13, CMA-13110, CMC-13110 and CMT-13110 have Co:Mo molar ratio of 1:3 and Mo:support molar ratio of 1:10. 4,6-DMDBT concentration of model diesel was 10 ppm which is the current sulfur content limit of commercial diesel fuels.

Table 1 – HDS activity of catalysts (50 bar and 2.1 hr^{-1}).

Catalysts	Removing efficiency of 4, 6-DMDBT (%)	
	Temperature (°C)	
	350	400
Commercial $CoMo/Al_2O_3$	85.2	97.7
CMO-13	29.6	95.4
CMA-13110	93.8	99.2
CMC-13110	99.1	99.6
CMT-13110	82.1	69.9

The performance of catalysts for HDS process was evaluated by concentration of 4, 6-DMDBT. The desulfurized model diesels were analyzed by GC-SCD and the results are summarized in Table 1. Catalytic activities were evaluated using the removing efficiency of 4, 6-DMDBT. The removing efficiency of 4, 6-DMDBT was calculated as $(C_i-C_o)/C_i$ where C_i is an initial concentration of 4, 6-DMDBT and C_o is a concentration of 4, 6-DMDBT at the reactor outlet.

The removing efficiency of 4,6-DMDBT with CMA-13110, CMC-13110 and CMT-13110 at LHSV of 2.1 hr^{-1} were 93.8%, 99.1% and 82.1%, respectively, at 350 °C and 99.2%, 99.6% and 69.9%, respectively, at 400 °C. Removing efficiency of 4, 6-DMDBT by commercial $CoMo/Al_2O_3$ at 350 °C and 400 °C were 85.2% and 97.7%, respectively. Among synthesized catalysts, CMC-13110 showed highest removing efficiency of 4,6-DMDBT. The remained concentrations of 4,6-DMDBT after desulfurization with CMC-13110 at 350 °C and 400 °C are 0.09 ppm and 0.04 ppm, respectively and less than target (<0.1 ppm). In the case of CMA-13110 at 400 °C, remained concentrations of 4, 6-DMDBT is 0.08 ppm and less than target.

CMA-13110 and CMC-13110 shows better performance than commercial $CoMo/Al_2O_3$. As shown in Fig. 16(d), the Raman spectra of CMC-13110 presents that the mixture of $CoMoO_4$ phase (939 cm^{-1}), γ-$Ce_2Mo_3O_{13}$ phase (767 cm^{-1}), and Mo cluster (700 cm^{-1}) were dominant. The Raman spectra of CMA-13110 showed characteristic broad bands of Mo=O vibration (995 cm^{-1}), and asymmetric Mo-O-Mo stretching vibrations (819 and 375 cm^{-1}). These broad spectra and oxygen vacancy increase catalytic activity.

However, CMT-13110 and CMO-13 showed poor catalytic activity. TiO_2 made CMT-13110 have different morphology from initial TiO_2. However, The Raman spectrum of CMT-13110 in Fig. 16(e) is very similar with the Raman spectrum of CMO-13 with the peak of 995 cm^{-1}, 819 cm^{-1}, 666 cm^{-1}, 336 cm^{-1}, and 290 cm^{-1} TiO_2 has lass effect on the catalytic activity.

From the removing efficiency of 4, 6-DMDBT after desulfurization, it was found that CMC-13110 ($CoMo/CeO_2$) was the most effective HDS catalyst. As a result, the desulfurized diesel using CMC-13110 (at 50 bar, with LHSV of 2.1 hr^{-1}, and temperatures of 350 and 400 °C) can be used in the reforming process for fuel cell applications.

Conclusion

Six catalysts, one commercial $CoMo/Al_2O_3$ and five catalysts made from USP were characterized and applied to HDS. The catalysts prepared by USP had Co:Mo molar ratio of 1:3 and Mo:support molar ratio of 1:10. The supports used were Al_2O_3, CeO_2, and TiO_2. For all support cases (Al_2O_3, CeO_2, TiO_2), we found that the Co and Mo particles are uniformly distributed on the supports, which was confirmed by SEM and EPMA measurements. The studies of surface properties displayed the formation of characteristic phases in each synthesized catalyst: (1) MoO_3 and $CoMoO_4$ phases for the $CoMo/Al_2O_3$ case (2) $Ce_2Mo_3O_{13}$, MoO_3, $CoMoO_4$ and Mo cluster phases for the $CoMo/CeO_2$ case (3) MoO_3 phase for the $CoMo/TiO_2$ case. HDS experiments were carried out at 50 bar, with LHSV of 2.1 hr^{-1}, and temperatures of 350 and 400 °C using a flow reactor in order to evaluate the activity of prepared catalysts toward HDS. Model diesel made from 4, 6-DMDBT and dodecane was used for accurate analysis of sulfur removal. We found that the catalyst using CeO_2 as support (CMC-13110) showed the highest catalytic activity, reducing the amount of 4, 6-DMDBT from 10 ppm to 0.09 ppm and 0.04 ppm at 350 °C and 400 °C, respectively. To conclude, $CoMo/CeO_2$ produced from USP was capable of desulfurizing 4, 6-DMDBT to less than 0.1 ppm, making it suitable for fuel cell applications.

Acknowledgment

This work was financially supported by the Renewable Energy R&D Program (No. 20133030030650) of the Korea Institute of Energy Technology Evaluation and Planning (KETEP), the Global Research Laboratory Program funded by the Ministry of Education, Science and Technology of Korea and the KIST institutional program (No. 2E26590) for the Korea Institute of Science and Technology.

Appendix A. Experimental set-up

The schematic figure of the USP process is shown in Fig. A1. The USP process consists of a preheater (1.5 kW, VFS Heater, ThermAll System), a main heater (4.6 kW, VFS Heater, ThermAll System), and an atomizer (Dong Lim Co. 1.7 MHz Ultrasonic). The preheater was maintained at 150 °C to evaporate the solvent of the precursor solution. The main heater was kept at 500 °C to crystallize the precursor solution. Produced powders were collected using a thimble filter (2.4 × 100 mm, ADVANTEC). The carrier gas was air with a flow rate of 1.5 ml/min.

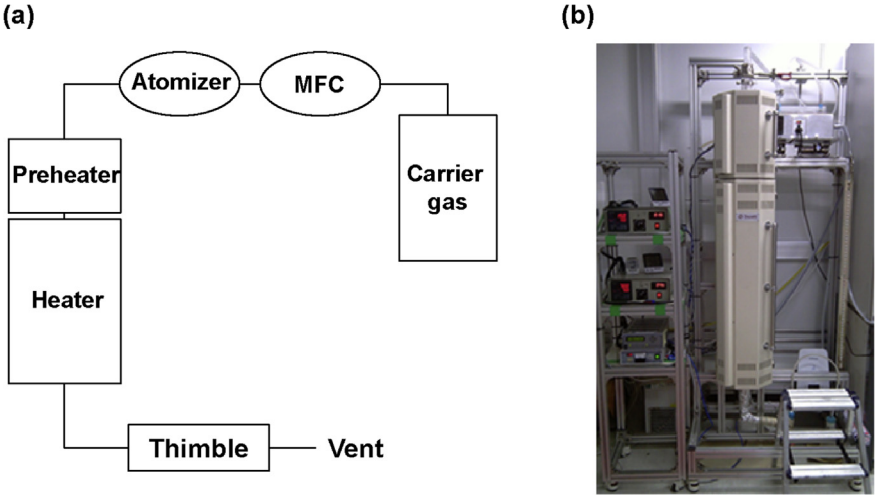

Fig. A1 – Ultrasonic spray pyrolysis (USP) process: (a) Schematic figure and (b) Experimental set-up.

The schematic figure and the experimental set-up are shown in Fig. A2(a) and (b), respectively. The HDS process uses a tubular reactor, a mass flow controller (MFC), and a back-pressure regulator (BPR). In the tubular reactor, 2.3 g of prepared catalysts were placed and tightly sealed for the HDS reaction. The reactor was pressurized to the desired pressure using the BPR located at the reactor exit, and finally heated to the desired temperature. When the desired temperature and pressure were reached, model diesel was pumped into the reactor using a high pressure pump (HPLC Series II Pump).

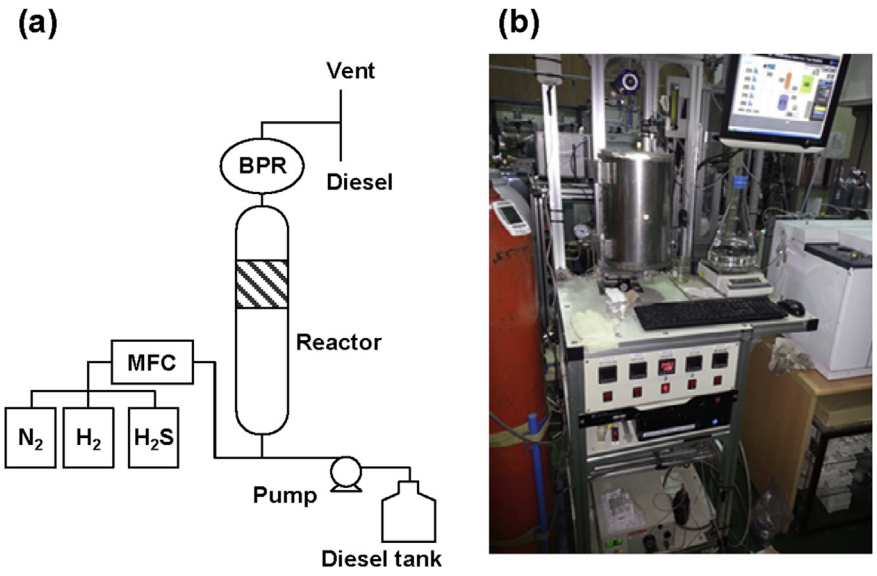

Fig. A2 – Hydrodesulfurization process: (a) Schematic figure and (b) Experimental set-up.

REFERENCES

[1] Bensaid S, Specchia S, Federici F, Saracco G, Specchia V. MCFC-based marine APU: comparison between conventional ATR and cracking coupled with SR integrated inside the stack pressurized vessel. Int J Hydrogen Energy 2009;34(4):2026–42.

[2] Lim SM, Kim J-N, Park J, Han SS, Park J-H, Jung TS, et al. Energy-efficient sulfone separation process for the production of ultralow sulfur diesel by two-step adsorption. Energy & Fuels 2012;26(4):2168–74.

[3] Martin S, Kraaij G, Ascher T, Baltzopoulou P, Karagiannakis G, Wails D, et al. Direct steam reforming of diesel and diesel–biodiesel blends for distributed hydrogen generation. Int J Hydrogen Energy 2015;40(1):75–84.

[4] Antolini E. The stability of molten carbonate fuel cell electrodes: a review of recent improvements. Appl Energy 2011;88(12):4274–93.

[5] Walluk MR, Lin J, Waller MG, Smith DF, Trabold TA. Diesel auto-thermal reforming for solid oxide fuel cell systems: anode off-gas recycle simulation. Appl Energy 2014;130(:94–102.

[6] Campanari S, Manzolini G, Chiesa P. Using MCFC for high efficiency CO2 capture from natural gas combined cycles: comparison of internal and external reforming. Appl Energy 2013;112(:772–83.

[7] Srivastav A, Srivastava VC. Adsorptive desulfurization by activated alumina. J Hazard Mater 2009;170(2):1133–40.

[8] Otsuki S, Nonaka T, Takashima N, Qian W, Ishihara A, Imai T, et al. Oxidative desulfurization of light gas oil and vacuum gas oil by oxidation and solvent extraction. Energy & Fuels 2000;14(6):1232–9.

[9] Kabe T, Ishihara A, Qian W. Hydrodesulfurization and hydrodenitrogenation: chemistry and engineering. Wiley-VCH; 2000.

[10] Breysse M, Djega-Mariadassou G, Pessayre S, Geantet C, Vrinat M, Pérot G, et al. Deep desulfurization: reactions, catalysts and technological challenges. Catal Today 2003;84(3–4):129–38.

[11] Whitehurst DD, Isoda T, Mochida I. Present state of the art and future challenges in the hydrodesulfurization of polyaromatic sulfur compounds. 1998.

[12] Wu Y, Hu G, Xie Y, Guo M, Luo M. Solid state reaction of MoO3–CeO2 complex oxide studied by Raman spectroscopy. Solid State Sci 2011;13(12):2096–9.

[13] Eijsbouts S, van den Oetelaar LCA, van Puijenbroek RR. MoS2 morphology and promoter segregation in commercial Type 2 Ni–Mo/Al2O3 and Co–Mo/Al2O3 hydroprocessing catalysts. J Catal 2005;229(2):352–64.

[14] Bej SK, Maity SK, Turaga UT. Search for an efficient 4,6-DMDBT hydrodesulfurization catalyst: a review of recent studies. Energy & Fuels 2004;18(5):1227–37.

[15] Korányi TI, Manninger I, Paál Z, Marks O, Günter JR. Activation of unsupported Co–Mo catalysts in thiophene hydrodesulfurization. J Catal 1989;116(2):422–39.

[16] Choi K-H, Korai Y, Mochida I. Preparation and characterization of nano-sized CoMo/Al2O3 catalyst for hydrodesulfurization. Appl Catal A General 2004;260(2):229–36.

[17] Caceres C, Fierro JG, Lazaro J, Agudo AL, Soria J. Effect of support on the surface characteristics of supported molybdenum catalysts. J Catal 1990;122(1):113–25.

[18] Qabazard H, Abuseedo F, Stanislaus A, Andari M, Absihalabi M. Comparison between the performance of conventional and high-metal co-mo and ni-mo catalysts in deep desulfurization of Kuwait atmospheric gas oil. Fuel Sci Technol Int 1995;13(9):1135–51.

[19] Song C. An overview of new approaches to deep desulfurization for ultra-clean gasoline, diesel fuel and jet fuel. Catal Today 2003;86(1–4):211–63.

[20] Heegn H, Birkeneder F, Kamptner A. Mechanical activation of precursors for nanocrystalline materials. Cryst Res Technol 2003;38(1):7–20.

[21] Mazurelle J, Lamonier C, Lancelot C, Payen E, Pichon C, Guillaume D. Use of the cobalt salt of the heteropolyanion [Co2Mo10O38H4]6– for the preparation of CoMo HDS catalysts supported on Al2O3, TiO2 and ZrO2. Catal Today 2008;130(1):41–9.

[22] Mestl G, Srinivasan TKK. Raman spectroscopy of monolayer-type catalysts: supported molybdenum oxides. Catal Rev 1998;40(4):451–570.